Research Article

Hocine Mzad* and Fethi Bennour

Industrial gas turbine performance prediction and improvement – a case study

https://doi.org/10.1515/ehs-2022-0094
Received August 8, 2022; accepted April 11, 2023;
published online April 27, 2023

Abstract: The gas turbines (GTs), model M3142R/GE MS 3002, equipping the natural gas compression and crude oil pumping stations of SONATRACH's pipeline transport of hydrocarbons activity are robust despite their dilapidation and state of service, but mediocre in terms of energy efficiency and power output. According to the manufacturer, for temperatures ranging from 15 to 47 °C, the efficiency of these machines drops from 26.78 to 25.03 % and their power drops from 11.29 to 8.9191 MW. It should be noted, however, that the number of these turbines exceeds 80 units and that their operation dates from 1974. The intention of this paper is to improve the gas turbine performance, mainly the efficiency and shaft power, by an evaporative cooling process of the compressor intake air. Besides, it is proposed to lower the upper limit power in periods of high temperatures to reduce gas consumption. To achieve these objectives, a mathematical model was implemented under Matlab R16, which reproduced the real behavior of these machines. It follows that this simulation made it possible to highlight relevant gains in terms of power and efficiency of the order of 1.361 MW and 3.4 % at a temperature of 47 °C.

Keywords: efficiency; evaporative cooling; gaz turbine M3142R type; performance; prediction.

Nomenclature

C_p	specific heat, J/(kg K)
EGT	exhaust gas temperature
f	fuel-to-air flowrate ratio (without cooling)
f'	fuel-to-air flowrate ratio (with cooling)
h_v	water steam enthalpy, kJ/kg
h_{g1}	humid air enthalpy at compressor inlet, kJ/kg
NCV	net calorific value
PGR	power gain ratio
P	power, kW
p	pressure, Pa
p_{sat}	water steam saturation pressure, Pa
p_v	water steam partial pressure, Pa
Q_h	fuel supplied heat, kJ
q_a	air mass flow, kg/s
q_c	cooling mass flow, kg/s
q_f	fuel flowrate without evaporative cooler, kg/s
q'_f	fuel flowrate with evaporative cooler, kg/s
q_{NG}	natural gas mass flow, kg/s
r_c	compression ratio
r_t	expansion ratio
T	temperature, K
T_c	compressor temperature, K
T_{cr}	critical temperature, K
T_d	dew-point temperature, K
T_r	reduced temperature
T_w	wet-bulb temperature, K
TEC	thermal efficiency coefficient

Greek symbols

Δp	pressure drop, Pa
ϕ	relative humidity, %
p_{NG}	naturel gas density, kg/m^3
ω	relative humidity measured in kilograms of water per kilogram of air
η	efficiency
η_c	compressor efficiency
η_m	GT mechanical efficiency
η_t	turbine efficiency
γ_a	air average adiabatic exponent (between suction and discharge of the axial compressor)
γ_g	adiabatic exponent of hot gases

Subscripts

a	air
adm	admission

***Corresponding author: Hocine Mzad**, Mechanical Engineering Department, Badji Mokhtar University of Annaba, Annaba, P.O. Box 12, DZ-23005, Algeria, E-mail: h_mzad@yahoo.fr. https://orcid.org/0000-0001-9900-6960
Fethi Bennour, Mechanical Engineering Department, Badji Mokhtar University of Annaba, Annaba, P.O. Box 12, DZ-23005, Algeria; and Laboratory of Research on Industrial Risk Control and Safety, Badji Mokhtar University of Annaba, Annaba, P.O. Box 12, DZ-23005, Algeria. https://orcid.org/0000-0002-8778-3014

amb	ambient
atm	atmospheric
LP	low pressure
c	compressor
cc	combustion chamber
d	dew point
evap	evaporative cooling
GT	gas turbine
g	hot gas
g1	relative to saturated water vapor
HP	high pressure
wc	with cooling
woc	without cooling
sat	saturation
t	turbine
v	vapor (steam)
2	compressor outlet with cooling
3	combustor outlet and HP tunbine inlet
4	HP turbine outlet
5	LP turbine inlet

1 Introduction

Industrial gas turbines (GTs) are thermal machines with rotors developing high power to drive gas pipeline line gas compressors, oil pipeline line pumps, and alternators to produce electrical energy. These massive machines are constantly being improved, in particular the fluid flow or "creep point" to which the noble elements are subjected. The fixed and mobile blades are, for the most part, subject to extensive research given the stresses exerted and temperature levels.

However, gas turbines already in service have seen the emergence of technical solutions that can improve their reliability, service life and efficiency. These advances, the result of technological advances and CFD simulations, have the advantage of increasing the turbine inlet temperatures and ensuring better cooling of the fins. A retrofit of the noble components of the GT is carried out on old machines.

Turbine air inlet cooling is one of the available commercial methods to improve the efficiency of existing gas turbines. The method has various types of air cooling which could be utilized for almost all installed gas turbines. A new type of inlet air cooling has been proposed to improve the performance of a gas turbine (Farzaneh-Gord et al. 2009). The inlet air of the gas turbine was cooled by the potential cooling capacity of the isenthalpic pressure drop. The results show that the gas turbine inlet air temperature can be reduced by 4–25 K and performance can be improved by 1–3.5 % over a long period of time.

Aspiring to decrease the compressor inlet air temperature, Noroozian and Bidi (2016) replaced the pressure reduction valve in the natural gas pressure reduction station with a turbo-expander connected to a mechanical chiller to produce refrigeration. Results showed that using a cooling system causes a 3.2 % temperature drop, which leads to a 1.138 % increment in both thermal efficiency and net output power in the warmest month.

Vasserman and Shutenko (2017) proposed three methods of increasing the efficiency of steam, gas, and combined cycle power plants. Calculations have shown an increase in net efficiency of 20.1 % for steam turbine power plants, 12.8 % for gas turbine power plants, and 4.1 % for the steam part of combined cycle power plants.

A sensitivity analysis was performed for the latest H-class gas turbine in a simple cycle to predict the performance variation due to changes in design parameters (Kwon et al. 2019). The degree of increase in the combined cycle power was the largest when improving the turbine inlet temperature (TIT). When reheating and recuperation were adopted simultaneously, a cycle efficiency of 65 % was possible with an increase of 1% in both the compressor and turbine efficiencies.

Evaluations of three combined gas turbine cycle configurations, including innovative combinations, were executed according to the thermodynamics of conventional energy and exergy analysis (Khan and Tlili 2019). The effects of some combinations, including simple and regenerative gas turbine cycles, on the performance and the exergy destruction of the combined cycle power plant were investigated.

A thermal performance study was carried out on the MS7001 gas turbine with a nominal power of 87 MW using the exergy balance (Haouam et al. 2019). The results show that the exergy destruction of the gas turbine depends on the ambient temperature, the compression ratio and air-fuel proportions. The total exergy destruction achieved was 53.51 MW, with an efficiency of 32.44 %.

A simulation of water injection processes in 18 stationary gas turbines for five different cities was introduced (Salehi et al. 2020). The calculated operating results showed that the variation of the output parameters was highly sensitive to the ambient temperature, relative humidity, and turbine inlet temperature (TIT). Saturated fogging plus 1 % overspray leads to a relative increase of 24.84 % and 6.70 % in net power output and thermal efficiency, respectively.

Marin et al. have investigated a gas turbine of the GE 6FA model and created its mathematical model (Marin et al. 2020). They have studied the effect of fuel temperature on the energy and economic characteristics of the gas turbine by considering natural gas, synthesis gas, and aviation kerosene as fuel. Meanwhile, (Abudu et al. 2020) focus on the injection of compressed air to facilitate the improvement in the ramp-up rate of a heavy-duty gas turbine. The performed

simulations using the constant mass flow method show that the heavy-duty gas turbine ramp-up rate can be improved by 10 % on average for every 2 % of compressor outlet airflow injected during ramp-up irrespective of the starting load. The turbine entry temperature was found to be another restrictive factor at a high injection rate of up to 10 %.

The integration of vapor compressor inlet air cooling (VC-IAC) in a cooled gas turbine cycle has been reported to further enhance the plant's specific work and plant efficiency, notably in regions having a hot and dry climate. It has been observed that the plant specific work increased by more than 0.35 % and the plant efficiency increased by a little above 0.1 % for every 1 °C drop in compressor inlet temperature (CIT) (Mishra et al. 2021).

An extensive literature review has been conducted to illustrate the rotational effects on various gas turbine internal cooling schemes from recent experimental and numerical investigations (Yeranee and Rao 2021). Recommendations for future research were outlined based on analyses of the effects of rotation on different internal cooling schemes, the effects of the buoyancy parameter, and the rotational effects on the friction factors, respectively.

The six similar gas turbine power cycles were selected to be compared deeply, and the required parameters for monitoring a power plant were introduced and calculated (Golneshan and Nemati 2021). The results demonstrate the method's ability to improve cycle performance, providing valuable repair or maintenance guidelines if used on a regular basis.

An innovative version of a humidified gas turbine cycle was introduced as "Top Cycle" (Dybe et al. 2021). The concept of which includes the necessary combustion infrastructure to generate highly efficient power and heat from a large variety of fuels. Operation at design conditions results in electric efficiencies higher than 50 % and power densities higher than 2100 kW per kg of air.

Gas turbine efficiency can be improved in several ways. Controlling the humidity and temperature of the air entering the combustion cycle is one of the most important points since it has a direct effect on the efficiency, emissions and operational reliability of the turbine.

This is the purpose of this work through the study of the GE MS 3002 Frame 3R turbine installed in the pumping and compression stations of SONATRACH, an Algerian oil and gas company. A simulation was performed to predict the effects of evaporative cooling on turbine performance.

2 Efficiency improvement at the axial compressor inlet

Reducing natural gas consumption by maintaining constant gas turbine power is achieved by practical processes that can be implemented on operating turbines. Indeed, under ISO conditions (T_{amb} = 15 °C, ϕ = 60 %, and p_{atm} = 1.0132 bar), the energy efficiency of gas turbines is typically 26 %. However, this efficiency is compromised by the conditions of high ambient temperatures and humidity. The average temperature in southern Algeria, especially during the summer, is around 45 °C, with daily maximums reaching 50 °C and relative humidity ranging from 10 to 20 %.

The actual power increase attributed to ambient air cooling depends on the machine model, temperature, ambient pressure, and relative humidity. This cooling generates the heat rate drop and therefore a diminution in the fuel flow consumption (Figure 1). On the other hand, high humidity increases the need for heat in the combustion chamber due to the high specific heat of water. Typically, for every 1 °C increase in ambient temperature, the power output of a gas turbine engine is reduced by approximately 0.5 % to 0.9 % (Alhazmy and Najjar 2004).

2.1 Evaporative cooling of intake air

Traditional water evaporative coolers have been widely used in the gas turbine industry for many years, particularly in hot climates with low humidity. The rational total cost of the installation and operating fees made this solution attractive for several GT situations in order to improve their performance.

The direct evaporative cooling process is basically based on the principle of converting sensible heat into latent heat. Ambient air is cooled by the evaporation of water from the wetted surface. Adding water vapor to the air increases its latent heat and relative humidity. If the process is adiabatic, this increase in latent heat is compensated by a reduction in the dry air temperature.

Isenthalpic evaporative coolers work on the principle of vaporizing water on a wall (media) made of corrugated fiber material. The water in the air evaporates as air passes through the media (Figure 2), releasing heat equal to the latent heat of vaporization (2500 kJ/kg at 0 °C). This process will naturally decrease the air temperature at the

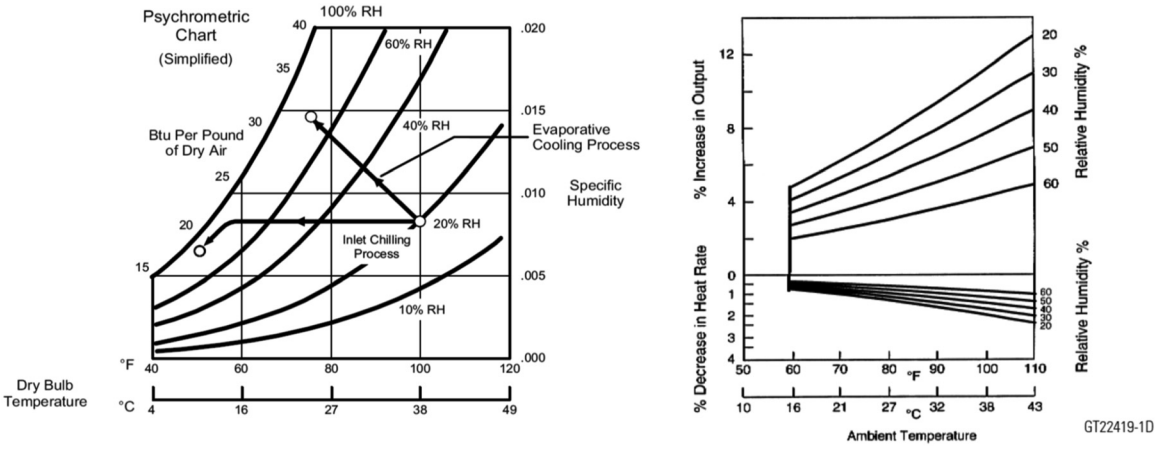

Figure 1: Psychrometric chart at the GT inlet (on the left). On the right-hand side, the influence of temperature and relative humidity on the GT power (White 1998).

compressor inlet. This technique is very effective in hot regions with low humidity. However, the water must be demineralized and free of salts, calcium, magnesium, and aluminum because contaminants act as electrolytes in humid air and cause severe corrosion. It should be noted that this method of improving the effective power is not expensive, and the temperature is lowered by 10 °C if the ambient temperature is around 32 °C.

2.2 Presentation of the gas turbine M3142R/ GE MS 3002

The studied gas turbine (GT), which has been manufactured in Germany since 1969, is a type of heavy-duty gas turbine (frame 3), shown in Figure 3. This GT, with two shafts, develops a power of 11.29 MW and can be equipped with a regenerator. The first rotor is made up of the axial compressor and the HP expansion turbine. In normal operation, this assembly, supported by two bearings, rotates at an isochronous speed equal to 7100 rpm, so the compressor delivers a pressure of between 4.9 and 5.1 bars, depending on the ambient temperature and pressure. The second rotor, representing the LP free turbine, rotates at a variable speed for a maximum equal to 6500 rpm. These GTs, model M3142R, are installed (simple cycle) in the stations of crude oil pumping and natural gas compression, coupled either to pumps or centrifugal compressors. The operating parameters of this GT model are summarized in Table 1. These values are used in the simulation section as a basis for calculations.

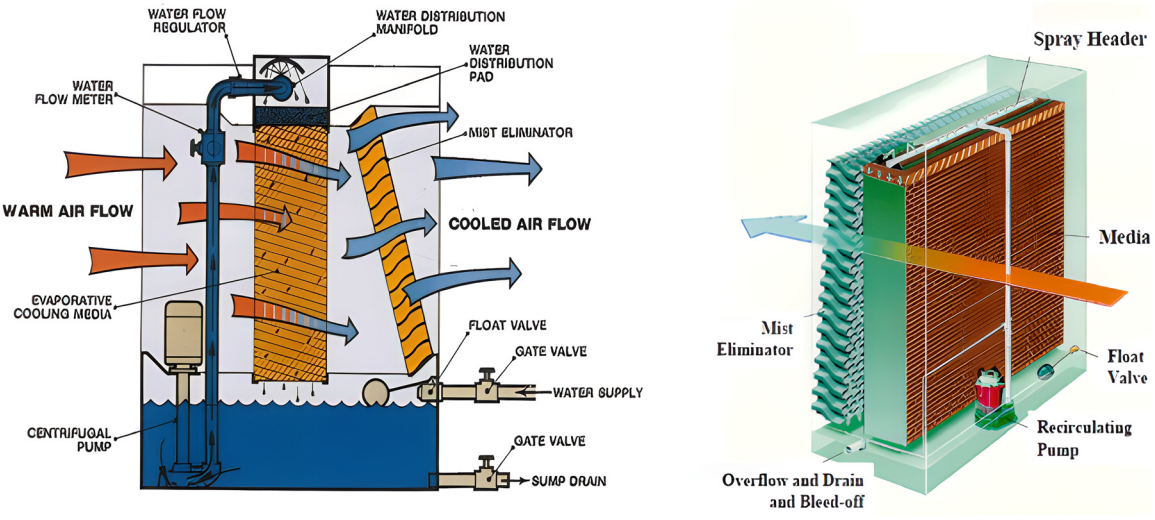

Figure 2: Working principle of the evaporative cooler (Donaldson Company 2020).

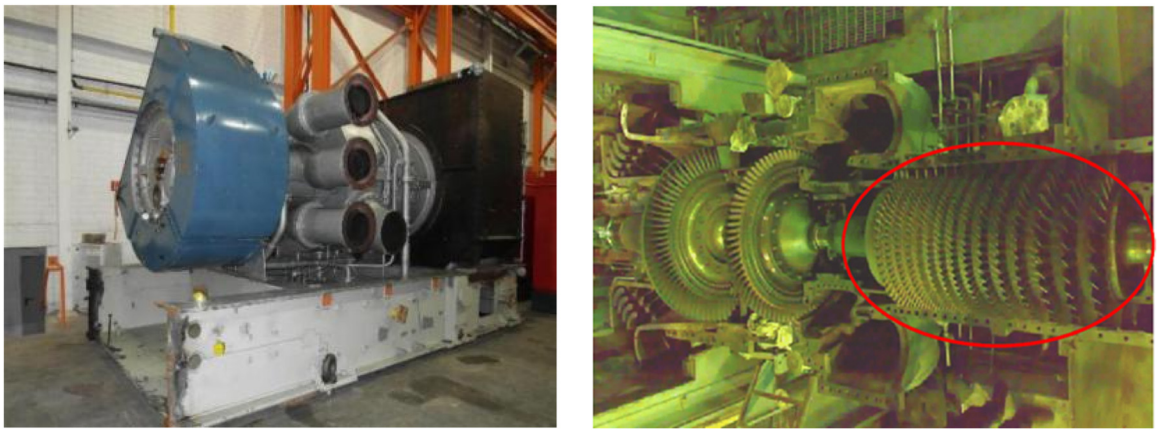

Figure 3: The gas turbine M3142R/GE MS 3002 frame 3R and the 15-stage compressor.

Table 1: The technical parameters of the GT (model M3142R/GE MS 3002).

q_a (kg/h)	q_c (kg/h)	η_t	η_c	η_m	η_{cc}	η_{GT}	NCV (kJ/kg)	Turbine stages
190,800	5200	0.88	0.92	0.95	0.95	25 %	45,119	15
EGT	T_{cc}	T_{amb}	Δp_{adm}	Δp_{cc}	p_{atm} (bar)	r_c	P (MW)	Heat rate (kJ/kWh)
542 °C	954 °C	0–50 °C	1 %	4 %	1.0132	6.1	11.290	13,440

The Table (Table 2), taken from the manufacturer's performance curves, shows the evolution of power, efficiency, and natural gas flow when the compressor inlet temperature rises from 15 to 47 °C. It appears that the power and efficiency of the GT drop by 2370.9 kJ/kWh and 1.75 %, respectively, but with lower fuel consumption. Moreover, the changes in gas turbine useful power and efficiency as a function of ambient temperature, assumed as the compressor inlet temperature, are illustrated graphically (Figure 4).

Table 2: Evolution of the GT efficiency as a function of compressor inlet temperature (ρ_{NG} = 0.78 kg/cm^3).

T_{inc} (°C)	P (kW)	Heat rate (kJ/kWh)	q_a (kg/s)	r_c	η_{GT} (%)	q_{NG} (kg/s)	q_a/q_f
15	11,290	13,440	53	6	26.78	0.936	55.56
20	10951,3	13574,4	52.21	6	26.52	0.917	55.86
25	10556,1	13708,8	51.41	6	26.26	0.893	56.48
30	10,161	13843,2	50.88	6	26	0.868	57.51
35	9822.3	13977,6	50.09	6	25.75	0.847	58.02
40	9427.1	14179,2	49.29	6	25.38	0.825	58.62
45	9144.9	14273,2	48.76	6	25.22	0.806	59.35
47	8919.1	14380,8	48.23	6	25.03	0.792	59.75

3 Mathematical formulation

A mathematical model was developed to predict the thermodynamic performance of M3142R type GTs as a function of ambient parameters such as ambient temperature and relative humidity. The influence of these parameters was analyzed by highlighting the contribution of evaporative cooling in terms of improving the energy efficiency of the studied GT (Figure 5).

The axial compressor inlet air mass flow highly influences the useful power. It depends on the ambient temperature and the relative humidity of the air. At ISO conditions,

$$q_a = \frac{q_{aISO}}{\rho_{ISO}} \rho_{(p,T_{amb},\omega_{amb})} = \frac{53}{1.212} \rho_{(p,T,\omega_{amb})} = 43.729\, \rho_{(p,T,\omega_{amb})} \quad (1)$$

with,

$$\rho_{(p,T,\omega_{amb})} = \frac{p_{atm}}{T_{amb}(0.287 + 0.462\omega_{amb})} \quad (2)$$

and,

$$\omega_{amb} = \frac{0.622\, p_v}{p_{atm} - p_v} = \frac{0.622\, p_{sat}\phi}{p_{atm} - p_{sat}\phi} \quad (3)$$

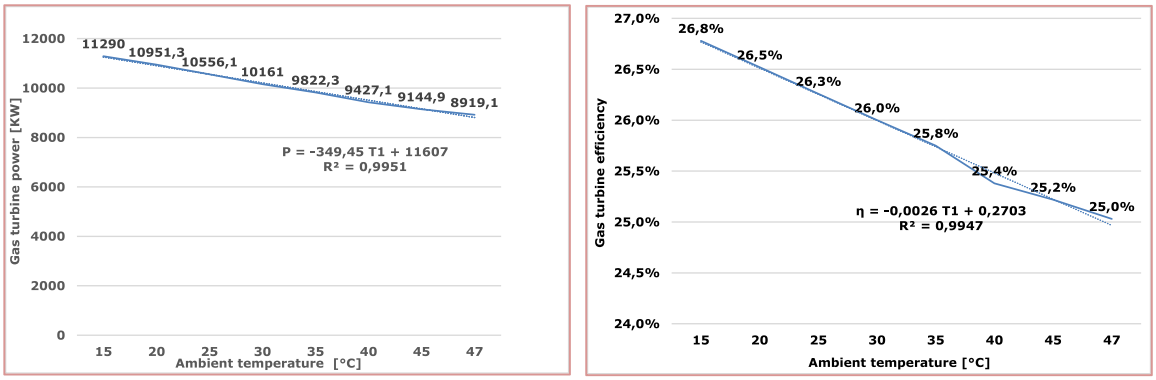

Figure 4: The evolution of GT power and efficiency with temperature.

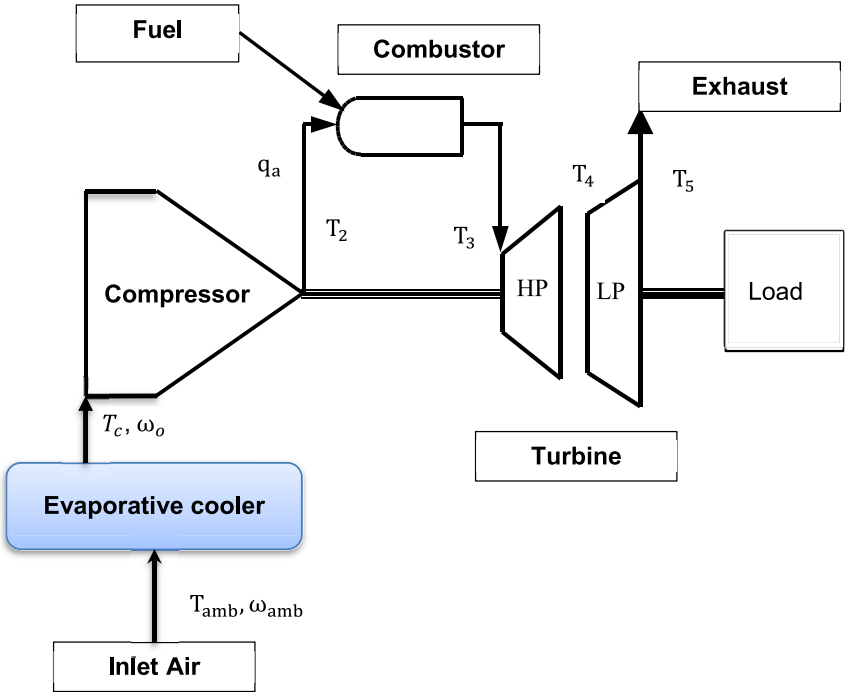

Figure 5: Simple-cycle two shafts gas turbine fitting the Algerian gas natural compressors stations (variable load).

According to (Hyland and Wexler 1983) and (Kim et al. 2004), the water vapor saturation pressure is:

$$p_{sat} = \exp\left[\frac{c_1}{T} + c_2 + c_3 T + c_4 T^2 + c_5 T^3 + c_6 \ln(T)\right] \quad (4)$$

with

$$c_1 = -5800.2206, c_2 = 1.3914993,$$

$$c_3 = -4.8640239\,10^{-2}, c_4 = 4.1764768 \times 10^{-5}$$

$$c_5 = -1.4452093 \times 10^{-8}, c_6 = 6.5459673$$

The outlet humidity ratio ω_o from the evaporative cooler is expressed as follows:

$$\omega_o = \omega_{sat} = \frac{0.622\, p_{sat}}{p_{atm} - p_{sat}} = \frac{0.622 \exp\left[\frac{c_1}{T_w} + c_2 + c_3 T_w + c_4 T_w^2 + c_5 T_w^3 + c_6 \ln(T_w)\right]}{p_{atm} - \exp\left[\frac{c_1}{T_w} + c_2 + c_3 T_w + c_4 T_w^2 + c_5 T_w^3 + c_6 \ln(T_w)\right]} \quad (5)$$

In the case of adiabatic process, the evaporative cooler delivers air to the compressor with a 100 % relative humidity (saturated air). The air temperature drops to the wet bulb temperature when the air passes through the water-spraying cooler. Hence, according to ASHRAE (Owen 2017), the equilibrium equation is written:

$$\omega_{amb}\,(2501 + 1.86\,(T - 273.15) - 4.186\,(T_w - 273.15)) = (2501 - 2.326\,(T_w - 273.15))\,\omega_o - 1.006\,(T - T_w) \quad (6)$$

The previous non-linear equation is computed using the Newton-Raphson algorithm under a Matlab code to determine the wet-bulb temperature T_w.

To check that no condensation occurs inside the axial compressor, the dew-point temperature is estimated by the Pepper's relation (Peppers 1988):

$$T_d = 6.54 + 14.526\,\ln(0.01p_v) + 0.7389\,(\ln(0.01p_v))^2 + 0.09486\,(\ln(0.01p_v))^3 + 0.4569\,(0.01p_v)^{0.1984} \quad (7)$$

The specific enthalpy of saturated vapor between 5 °C and 370 °C is estimated, with a maximum error of 0.13 % (3.2 kJ/kg), by the equation of Affandi et al. (2013):

$$\ln(h_g) = \sqrt{a + b\left[\ln\left({}^{1}/_{T_r}\right)\right]^{0.35} + c/{T_r}^2 + d/{T_r}^3 + e/{T_r}^4} \quad (8)$$

with,

$$a = 64.87678,\ b = 11.76476,\ c = -11.94431,\ d = 6.29015,\ e = -0.99893$$

T_r is the reduced temperature, which is defined as T/T_{cr}. The critical temperature (T_{cr}) for steam is 647.096 K (Wagner and Pruss 1993).

Considering the evaporative cooler efficiency equation (Owen 2017), the compressor temperature is estimated as follows:

$$T_c = \eta_{\text{evap}}\,(T_w - T_{\text{amb}}) + T_{\text{amb}} \quad (9)$$

The compressor outlet temperature when the process is isentropic is calculated as:

$$T_2 = T_c\left[1 + \frac{\left(r^{\frac{\gamma_a - 1}{\gamma_a}} - 1\right)}{\eta_c}\right] \quad (10)$$

The needed power by the compressor to heat the air and vapor water is given by:

Without cooling,

$$P_c = \frac{q_a}{\eta_m}\left[C_{pa}\,\frac{T_{\text{amb}}}{\eta_c}\left(r^{\frac{\gamma_a - 1}{\gamma_a}} - 1\right) + \omega_{\text{amb}}\,(h_{v2} - h_{g1})\right] \quad (11)$$

with cooling,

$$P_c = \frac{q_a}{\eta_m}\left[C_{pa}\,\frac{T_c}{\eta_c}\left(r^{\frac{\gamma_a - 1}{\gamma_a}} - 1\right) + \omega_o\,(h_{v2} - h_{g1})\right] \quad (12)$$

and the compression power of the humidified air is:

$$P_c = \frac{q_a}{\eta_m}\left[C_{pa}\frac{T_c}{\eta_c}\left(r^{\frac{\gamma - 1}{\gamma}} - 1\right) + \omega_{sat}\,(h_{v2} - h_{g1})\right] \quad (13)$$

The specific heat of dry air is given by the relation of Alhazmy and Najjar (2004):

$$C_{pa} = 1018.9134 - 0.13783636\,T + 1.9843397 \times 10^{-4}\,T^2 + 4.2399 \times 10^{-7}\,T^3 \quad (14)$$

Water vapor specific enthalpy at the outlet of an axial compressor according to ASHRAE (Owen 2017) is:

$$h_{v2} = 2501 + 1.86\,T_2 \quad (15)$$

According to the scheme (Figure 6), the energy balance equation in the combustor without evaporative cooling yields:

$$q_f\,NCV\,\eta_{cc} + q_a\,(C_{pa}\,(T_2 - T_{amb}) + \omega_{amb}\,(h_{v2} - h_{g1})) = (q_f + q_a)\,C_{pg}\,(T_3 - T_2) + q_a\,\omega_{amb}\,(h_{v3} - h_{v2}) \quad (16)$$

The effect of ambient humidity on the energy balance equation was ignored.

In gas turbines, it is commonly known that 90 % of the compressed air goes to the combustor, and 10 % is used for the bearings' sealing and hot parts' cooling. So, in Eq. (16), the air flow rate q_a becomes 0.9 q_a.

$$q_f\,NCV\,\eta_{cc} + 0.9q_a\,(C_{pa}\,(T_2 - T_{amb}) + \omega_{amb}\,(h_{v2} - h_{g1})) = (0.9\,q_f + q_a)\,C_{pg}\,(T_3 - T_2) + 0.9\,q_a\,\omega_{amb}\,(h_{v3} - h_{v2}) \quad (17)$$

The fuel flow rate consumed by the GT without evaporative cooling is estimated by the following formula:

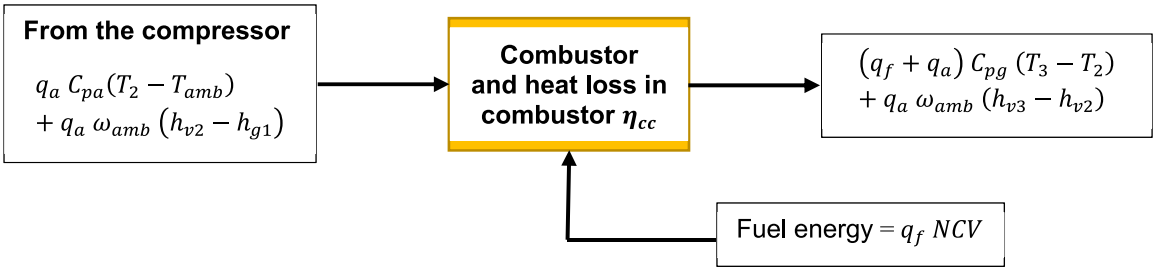

Figure 6: Energy balance in the combustor without evaporative cooling.

$$q_f = 0.9\,q_a \frac{C_{pg}\left(T_3 - T_{\text{amb}}\left(1 + \frac{(r^{\frac{\gamma_a-1}{\gamma_a}}-1)}{\eta_c}\right)\right) - C_{pa}T_{\text{amb}}\,\frac{(r^{\frac{\gamma_a-1}{\gamma_a}}-1)}{\eta_c} + \omega_{\text{amb}}\,(h_{v3} - 2\,h_{v2} - h_{g1})}{NCV\,\eta_{cc} - C_{pg}\left(T_3 - T_{\text{amb}}\left(1 + \frac{(r^{\frac{\gamma_a-1}{\gamma_a}}-1)}{\eta_c}\right)\right)} \tag{18}$$

The fuel-to-air flow rate ratio for the GT without an evaporative cooler is expressed as:

$$f = \frac{q_f}{q_a} = 0.9 \times \frac{C_{pg}\left(T_3 - T_{\text{amb}}\left(1 + \frac{(r^{\frac{\gamma_a-1}{\gamma_a}}-1)}{\eta_c}\right)\right) - C_{pa}\,T_{\text{amb}}\,\frac{(r^{\frac{\gamma_a-1}{\gamma_a}}-1)}{\eta_c} + \omega_{\text{amb}}\,(h_{v3} - 2\,h_{v2} - h_{g1})}{NCV\,\eta_{cc} - C_{pg}\left(T_3 - T_{\text{amb}}\left(1 + \frac{(r^{\frac{\gamma_a-1}{\gamma_a}}-1)}{\eta_c}\right)\right)} \tag{19}$$

when installing an evaporative cooler (Figure 7), the energy balance equation in the combustor is given by Eq. (20).

$$q_f' NCV\,\eta_{cc} + 0.9\,q_a\,C_{pa}\,(T_2 - T_c) + 0.9\,q_a\,\omega_o\,(h_{v2} - h_{g1}) = \left(q_f' + 0.9\,q_a\right) C_{pg}\,(T_3 - T_2) + 0.9\,q_a\,\omega_o\,(h_{v3} - h_{v2}) \tag{20}$$

The water vapor enthalpy is given by:

$$h_{v3} = 2501 + 1.86\,T_3 \tag{21}$$

With evaporative cooling, air is sucked from the cooler so that the outlet temperature of the cooler is T_c. For safety reasons inherent to the type of GT investigated, the temperature T_3 is kept equal to 954 °C to avoid the thermal creep of the HP rotor blades. The fuel flow rate consumption is calculated as follows:

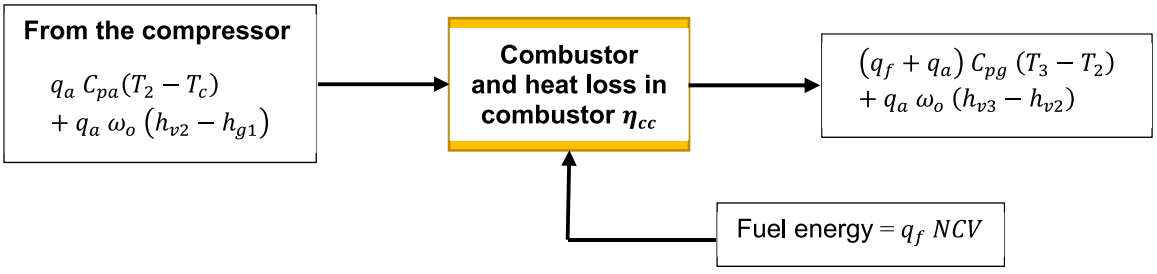

Figure 7: Energy balance in the combustor with evaporative cooling.

$$q_f' = 0.9\, q_a \frac{C_{pg}\left(T_3 - T_c\left(1 + \frac{\left(r^{\frac{\gamma_a-1}{\gamma_a}}-1\right)}{\eta_c}\right)\right) - C_{pa}\, T_c\, \frac{\left(r^{\frac{\gamma_a-1}{\gamma_a}}-1\right)}{\eta_c} + \omega_o\,(h_{v3} - 2h_{v2} - h_{g1})}{NCV\,\eta_{cc} - C_{pg}\left(T_3 - T_c\left(1 + \frac{\left(r^{\frac{\gamma_a-1}{\gamma_a}}-1\right)}{\eta_c}\right)\right)} \tag{22}$$

The fuel-to-air flow rate ratio for the GT with a cooling process at constant combustion temperature is written as:

$$f' = \frac{q_f'}{q_a} = 0.9 \frac{C_{pg}\left(T_3 - T_c\left(1 + \frac{\left(r^{\frac{\gamma_a-1}{\gamma_a}}-1\right)}{\eta_c}\right)\right) - C_{pa}\, T_c\, \frac{\left(r^{\frac{\gamma_a-1}{\gamma_a}}-1\right)}{\eta_c} + \omega_o\,(h_{v3} - 2h_{v2} - h_{g1})}{NCV\,\eta_{cc} - C_{pg}\left(T_3 - T_c\left(1 + \frac{\left(r^{\frac{\gamma_a-1}{\gamma_a}}-1\right)}{\eta_c}\right)\right)} \tag{23}$$

The gas specific heat (C_{pg}) is calculated by the following correlation (Owen 2017):

$$\begin{aligned} C_{pg} = {} & 1088.7572 - 0.14158834\ T + 1.9160159 \times 10^{-3}\ T^2 \\ & - 1.2400934 \times 10^{-6}\ T^3 + 3.0669459 \times 10^{-10}\, T^4 \\ & - 2.6117109 \times 10^{-14}\ T^5 \end{aligned} \tag{24}$$

The air specific heat capacity in the combustion chamber is C_{pcc} = 1.177 kJ/(kg K) at 954 °C and 5 bar. According to Bouam (2009), the fuel heat released without a cooling process is:

$$\begin{aligned} Q_{hwoc} = 0.9\ q_a \Bigg[& (1+f)\, C_{pcc}\, T_3 + C_{pa}\, T_{amb}\left(\frac{r^{\frac{\gamma_a-1}{\gamma_a}}-1}{\eta_c}+1\right) \\ & + \omega_{amb}\,(h_{v3} - h_{v2})\Bigg] \end{aligned} \tag{25}$$

and the fuel heat released with a cooling process at the compressor suction is:

$$\begin{aligned} Q_{hwc} = 0.9\ q_a \Bigg[& (1+f')\, C_{pcc}\, T_3 + C_{pa}\, T_c\left(\frac{r^{\frac{\gamma_a-1}{\gamma_a}}-1}{\eta_c}+1\right) \\ & + \omega_o\,(h_{v3} - h_{v2})\Bigg] \end{aligned} \tag{26}$$

The power developed by the gas turbine HP rotor without and with cooling, respectively, is:

$$P_{HPwoc} = 0.9\, q_a\, \eta_t\, \eta_m\, (1 + f + \omega_{amb})\, C_{pg}\, (T_3 - T_4) \tag{27}$$

$$P_{HPwc} = 0.9\, q_a\, \eta_t\, \eta_m\, (1 + f' + \omega_o)\, C_{pg}\, (T_3 - T_4) \tag{28}$$

Substituting T_4 by its expression (isentropic process), Eq. (28) becomes:

$$P_{HPwc} = 0.9\, q_a \left[(1 + f' + \omega_o)\, C_{pg}\ \eta_t\, \eta_m \left(1 - r_{tHP}^{\frac{\gamma_g-1}{\gamma_g}}\right)\right] \times T_3 \tag{29}$$

In order to compute the expansion rate of hot gases over the rotor HP, we put $P_{HP} = P_c$ because the compressor consumes a part of the power generated in the HP turbine. Thus, the expansion rate equation of the HP turbine is:

$$r_{tHP}^{\frac{1-\gamma_g}{\gamma_g}} = 1 - \frac{C_{pa}\, \frac{T_c}{\eta_c}\left(r^{\frac{\gamma_a-1}{\gamma_a}}-1\right) + \omega_o\,(h_{v3} - h_{v2})}{0.9\, C_{pg}\,(1 + f' + \omega_o)\,\eta_m\,\eta_c\,\eta_t\,T_3} \tag{30}$$

and the LP turbine wheel expansion rate is calculated by:

$$r_{tLP} = \frac{r}{r_{tHP}} \tag{31}$$

The useful power of the LP turbine shaft is determined by the equation:

$$P_{LPwc} = 0.9\ \eta_t\, \eta_m\, q_a (1 + f' + \omega_o)\, C_{pg}\ (T_4 - T_5) \tag{32}$$

$$P_{LPwoc} = 0.9\ \eta_t\, \eta_m\, q_a (1 + f + \omega_{amb})\, C_{pg}\ (T_4 - T_5) \tag{33}$$

Replacing the temperatures T_4 and T_5 with their expressions, we obtain:

$$\begin{aligned} P_{LPwoc} = 0.9\ \eta_t\, \eta_m\, q_a \Bigg[& (1 + f + \omega_{amb})\, C_{pg} \\ & \left(1 - r_{tLP}^{\frac{1-\gamma_g}{\gamma_g}}\right)\left(\eta_t\left(r_{tHP}^{\frac{1-\gamma_g}{\gamma_g}} - 1\right) + 1\right)\Bigg] \times T_3 \end{aligned} \tag{34}$$

$$P_{LPwc} = 0.9\ \eta_t \eta_m q_a \left[(1 + f' + \omega_o) C_{pg} \left(1 - r_{tLP}^{\frac{1-\gamma_g}{\gamma_g}}\right)\left(\eta_t \left(r_{tHP}^{\frac{1-\gamma_g}{\gamma_g}} - 1\right) + 1\right)\right] \times T_3 \quad (35)$$

once all parameters have been determined, the GT global efficiency is merely computed by:

$$\eta_{GTwc} = \frac{P_{LPwc}}{NCV\, q_f} \quad (36)$$

$$\eta_{GTwoc} = \frac{P_{LPwoc}}{NCV\, q_f'} \quad (37)$$

Finally, the power gain ratio and the thermal efficiency coefficient are reported by Alhazmy et al. (Owen 2017):

$$PGR = \frac{P_{LPwc} - P_{LPwoc}}{P_{LPwoc}} \times 100 \quad (38)$$

$$TEC = \frac{\eta_{GTwc} - \eta_{GTwoc}}{\eta_{GTwoc}} \times 100 \quad (39)$$

4 Simulation and results discussion

Performance simulation of the GT model M3142R is carried out thanks to a program implemented under the code Matlab R16. The air flow, conditioned by the dimensional aspect of the machine, and the outlet temperature of the combustion chamber together define the useful power of the gas turbine. The combustion temperature is set at a value of 954 °C (machine safety limit value). The predictions attained allow us to analyze the behavior of this type of GT when there is a variation in ambient conditions.

The power absorbed by the axial compressor increases proportionally with temperature and relative humidity (Figure 8). An increase in relative humidity (ϕ) from 10 to 80 % leads to an increase in compression power from 11.93 MW to 12.02 MW when the ambient temperature is 25 °C and from 11.96 MW to 12.15 MW when T_{amb} = 40 °C. This results in excess power consumed by the compressor of 90 kW and 190 kW, respectively. However, if the ambient temperature changes from 25° to 40°, the compression power increases by 30 kW for a constant humidity of ϕ = 10 % and by 130 kW for a humidity fixed at 80 %.

From inspection of Figure 9, it appears how the evaporative cooler affects the compressor inlet temperature. For a constant humidity of ϕ = 10 %, the ambient temperature is reduced by 50 % (from 25 to 12.65 °C). When the humidity is set to ϕ = 80 %, the temperature drops only slightly (from 25 to 22.77 °C). It should be noted that for regions with a dry and hot climate like in southern Algeria (ϕ = 10 %, T_{amb} = 47 °C),

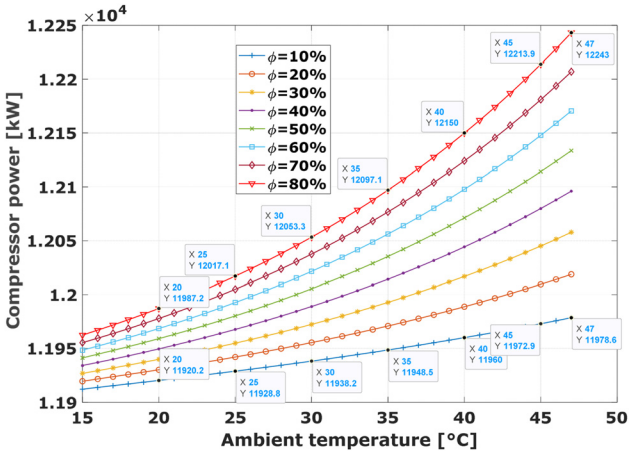

Figure 8: Compressor power progression without evaporative cooling.

the compressor inlet temperature drops considerably to T_{inc} = 25.93 °C, which makes it possible to improve the GT performance. On the other hand, in humid and hot regions (ϕ = 80 %, T_{amb} = 47 °C), evaporative cooling becomes almost ineffective since the temperature obtained is equal to 43.77 °C, which corresponds to a decrease of only 3.23 °C.

Figure 10 highlights the impact of ambient temperature and humidity on the power of the GT LP shaft. Noticeable power gains are observed if the temperature and humidity decrease. In southern Algeria, where an average temperature of 45 °C is recorded in summer, we can see on the curves the effect of the decrease in humidity on the improvement in power. Indeed, the curves indicate that if ϕ = 10 %, the power P_{LP} = 9.673 MW, whereas for ϕ = 80 %, the power P_{LP} = 8.312 MW, which means a power gain equal to 1.361 MW. Obviously, the evolution of efficiency (Figure 11) is in line with that of the previous power curves. When the temperature is 45 °C, the GT efficiency decreases from 0.2519

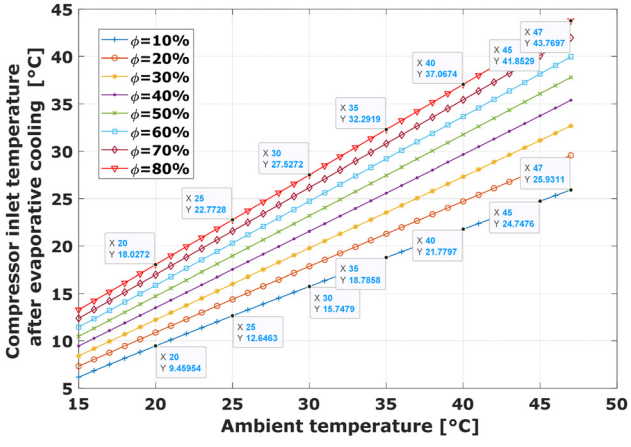

Figure 9: Effect of evaporative cooling on T_{inc}.

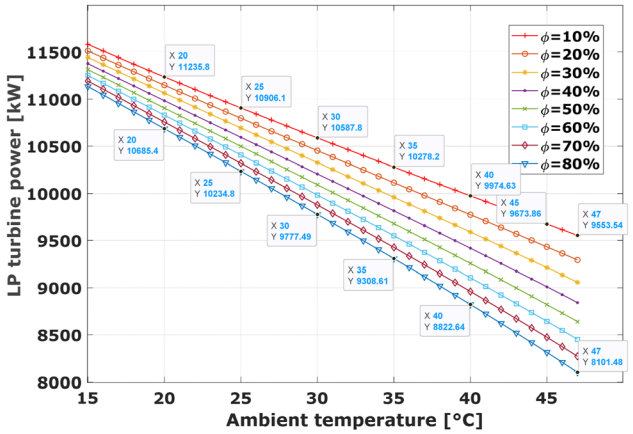

Figure 10: GT useful power progression with evaporative cooling.

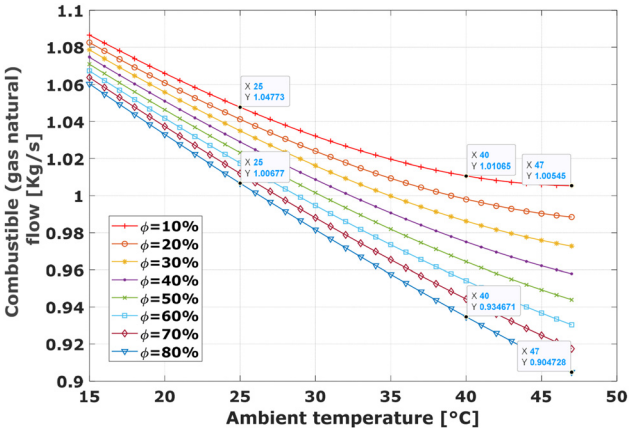

Figure 12: Fuel consumption as a function of ambient conditions.

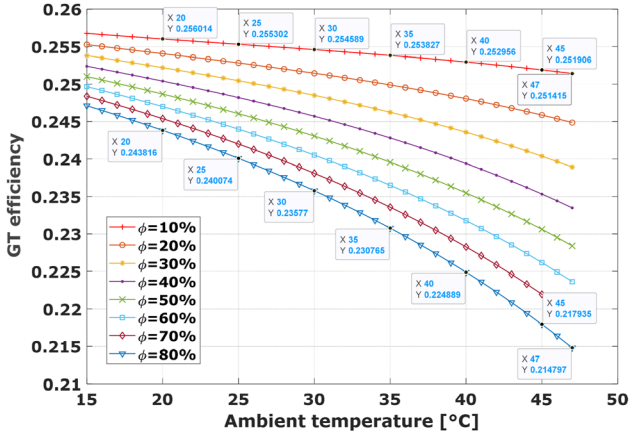

Figure 11: GT efficiency progression with evaporative cooling.

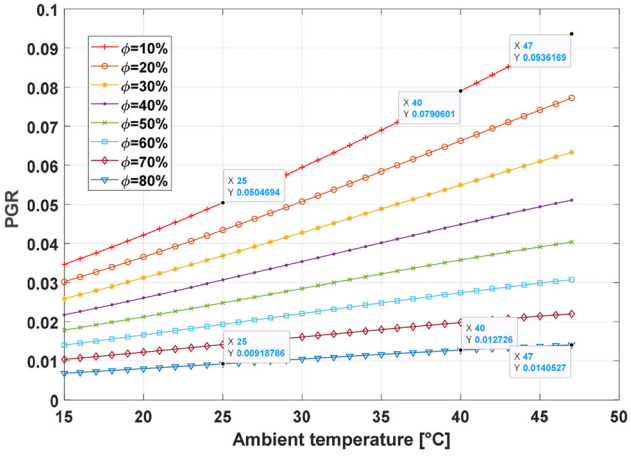

Figure 13: Power gain ration as a function of ambient conditions.

to 0.2179 as the humidity increases from 10 % to 80 %. This improvement in efficiency (+3.4 %) is due to the power of 1361 MW previously recovered by the LP impeller. Furthermore, it should be noted that the decrease in temperature from 45 to 25 °C has a weak influence on the output (+0.34 %) at low humidity (ϕ = 10 %). If, on the other hand, ϕ = 80 %, the output increases by 2.22 % from 0.2179 to 0.2401.

The gas turbine consumes less fuel (natural gas) when the temperature and humidity are high (Figure 12). When T_{amb} = 47 °C, the gas consumption drops from 1.005 kg/s to 0.9047 kg/s as humidity increases from 10 % to 80 %. At T_{amb} = 25 °C, consumption ranges from 1.048 kg/s (if ϕ = 10 %) to 1.007 kg/s (if ϕ = 80 %). As a result, using the evaporative cooling system requires additional energy from the fuel to bring the mixture to the cycle temperatures.

Finally, to assess the impact of the evaporative cooler on the performance improvement of the studied GT, we have illustrated in Figures 13 and 14 the trends of the power gain ratio (*PGR*) and the thermal efficiency coefficient (*TEC*). The results (Figure 13) illustrate the insignificant effect of ambient temperature on *PGR* when humidity is high (ϕ > 50 %). On the other hand, if the humidity is low (ϕ = 10 %), we note an increase in the *PGR* from 0.05047 to 0.09362, corresponding to the temperatures of 25 °C and 47 °C, respectively. The highest *PGR* values are recorded by the majority of SONATRACH stations during hot (40–47) °C and dry periods ($\phi \leq$ 10 %).

For relatively humid climates of the order of 40–80 %, there is a drop in thermal efficiency (Figure 14) of up to –3.7 % (at 80 %). The negative values of the *TEC* are due to an increase in fuel consumption necessary to vaporize the water contained in the intake air. The *TEC* improves from 30 % humidity at 40 °C, i.e., when approaching a dry climate, which is prevalent in the Saharan zones where the GTs. At this point, the evaporative cooler outlet temperature drops and the shaft LP power increases. When approaching 47 °C, a dry climate with a relative humidity of 10 % can result in a 4.85 % improvement in the *TEC*.

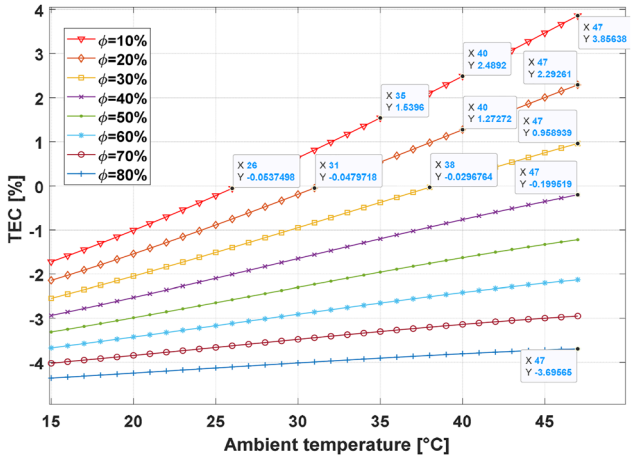

Figure 14: Thermal efficiency coefficient as a function of ambient conditions.

5 Conclusions

The industrial gas turbine model M3142R/GE MS 3002 is a thermodynamic rotating machine whose performance is the subject of continuous improvement studies. These robustly designed GTs deliver low efficiency (25–30 %) compared to new generation GTs. This is why we have tried, through this article, to study their combined behavior with respect to humidity and temperature and then try to improve their power, performance, and energy efficiency without additional gas consumption.

The study carried out for this purpose has enabled us to highlight relevant gains in useful power of the order of 1.361 MW, combined with an improvement in efficiency of 3.4 %, when these machines are operated at extreme temperatures of around 47 °C and a relative humidity of 10 %. The installation of an evaporative cooling system is an effective way to reduce the temperature at the suction of the axial compressor of the GT. Obviously, with low ambient humidity, the efficiency of the machine increases, which allows the turbine to recover part of the power that was intended, without this system, to drive the compressor.

Rightly, the procedure adopted for the evaluation of the effects of the installation of evaporative coolers can be applied to other higher-power GTs in service. We can mention the turbines used in the reinjection of water or gas at the level of hydrocarbon wells (GE 6000) or those used in thermal power stations for the production of electrical energy (GE 9000). Furthermore, in their research report (Brooks 2021), General Electric states that evaporative cooling systems are applicable to medium-power gas turbines such as the LM2500, LM6000, and LMS100 models.en

Author contributions: All the authors have accepted responsibility for the entire content of this submitted manuscript and approved submission.
Research funding: None declared.
Conflict of interest statement: The authors declare no conflicts of interest regarding this article.

References

Abudu, K., U. Igie, O. Minervino, and R. Hamilton. 2020. “Gas Turbine Efficiency and Ramp Rate Improvement through Compressed Air Injection.” *Journal of Power and Energy* 235 (4): 866–84.

Affandi, M., N. Mamat, S. N. Aqmariah Mohd Kanafiah, and N. S. Khalid. 2013. “Simplified Equations for Saturated Steam Properties for Simulation Purpose.” *Procedia Engineering* 53: 722–6.

Alhazmy, M. M., and Y. S. H. Najjar. 2004. “Augmentation of Gas Turbine Performance Using Air Coolers.” *Applied Thermal Engineering* 24 (2–3): 415–29.

Alhazmy, M. M., R. K. Jassim, and G. M. Zaki. 2006. “Performance Enhancement of Gas Turbines by Inlet Air-Cooling in Hot and Humid Climates.” *International Journal of Energy Research* 30 (10): 777–97.

Bouam, A. 2009. “Amélioration des performances des turbines à gaz utilisées dans l’industrie des hydrocarbures par l’injection de vapeur d’eau à l’amont de la chambre de combustion.” PhD thesis, M’hamed Bougara University.

Brooks, F. J. 2021. *GE Gas Turbine Performance Characteristics*, GE Power Systems Schenectady, NY. (accessed Auguest 30, 2021).

Donaldson Company, Inc. 2020. *Gas Turbine Systems*. Bloomington: Filtration solutions. https://www.donaldson.com/en-us/gas-turbine/ (accessed Auguest 30, 2021).

Dybe, S., M. Bartlett, J. Palsson, and P. Stathopoulos. 2021. “TopCycle: A Novel High Performance and Fuel Flexible Gas Turbine Cycle.” *Sustainability* 13: 651.

Farzaneh-Gord, M., M. Deymi-Dashtebayaz, and S. Hashemi-Marghzar. 2009. “Improving the Efficiency of an Industrial Gas Turbine by a Novel Inlet Air Cooling Method.” *Journal of the Energy Institute* 82 (3): 150–8.

Golneshan, A. A., and H. Nemati. 2021. “Comparison of Six Gas Turbine Power Cycle, a Key to Improve Power Plants.” *Mechanics and Industry* 22 (8). https://doi.org/10.1051/meca/2021005.

Haouam, A., C. Derbal, and H. Mzad. 2019. “Thermal Performance of a Gas Turbine Based on an Exergy Analysis.” *E3S Web of Conferences* 128: 01027.

Hyland, R. W., and A. Wexler. 1983. “Formulations for the Thermodynamic Properties of the Saturated Phases of H_2O from 175.15 K to 473.15 K.” *ASHRAE Transactions* 89 (2A): 500–19.

Khan, M. N., and I. Tlili. 2019. “New Approach for Enhancing the Performance of Gas Turbine Cycle: A Comparative Study.” *Results in Engineering* 2: 100008.

Kim, B. S., T. Kim, and K. Kim. 2004. “Predicting Potential Condensation at the inside Surface of the Glazed Curtain Wall of High-Rise Residential Buildings.” *Journal of Asian Architecture and Building Engineering* 3 (2): 267–74.

Kwon, H. M., S. W. Moon, T. S. Kim, D. W. Kang, J. L. Sohn, and J. Lee. 2019. “A Study on 65 % Potential Efficiency of the Gas Turbine Combined Cycle.” *Journal of Mechanical Science and Technology* 33: 4535–43.

Marin, G., D. Mendeleev, B. Osipov, and A. Akhmetshin. 2020. “Study of the Effect of Fuel Temperature on Gas Turbine Performance.” *E3S Web of Conferences* 178: 01033.

Mishra, A., A. Srivastava, and A. K. Mohapatra. 2021. "Sanjay, Effect of Ambient and Operating Parameters on the Performance Parameters of Cooled Gas Turbine Cycle." *AIP Conference Proceedings* 2341: 030003.

Noroozian, A., and M. Bidi. 2016. "An Applicable Method for Gas Turbine Efficiency Improvement. Case Study: Montazar Ghaem Power Plant, Iran." *Journal of Natural Gas Science and Engineering* 28: 95–105.

Owen, M. S. 2017. *ASHRAE Fundamentals Handbook, Chapter I.1: Psychrometrics*, SI and IP ed. Atlanta: W. Stephen Comstock.

Peppers V. W. 1988. *ASHRAE Handbook Fundamental (1997)*, Unpublished paper, ASHRAE, 6.9–10.

Salehi, M., H. Eivazi, M. Tahani, and M. Masdari. 2020. "Analysis and Prediction of Gas Turbine Performance with Evaporative Cooling Processes by Developing a Stage Stacking Algorithm." *Journal of Cleaner Production* 277: 122666.

Vasserman, A. A., and M. A. Shutenko. 2017. "Methods of Increasing Thermal Efficiency of Steam and Gas Turbine Plants." *Journal of Physics: Conference Series* 891: 012248.

Wagner, W., and A. Pruss. 1993. "International Equations for the Saturation Properties of Ordinary Water Substance. Revised According to the International Temperature Scale of 1990." *Journal of Physical and Chemical Reference Data* 22 (3): 783–7.

White, F. M. 1998. *Heat and Mass Transfer*. Massachusetts: Addison-Wesley.

Yeranee, K., and Y. Rao. 2021. "A Review of Recent Studies on Rotating Internal Cooling for Gas Turbine Blades." *Chinese Journal of Aeronautics* 34 (7): 85–113.